EEP-VOL 10-2, Advances in Electronic Packaging
ASME 1995

ANALYTICAL MODEL FOR SIMULATING THE THERMAL BEHAVIOR OF MICROELECTRONIC SYSTEMS

P. Teertstra, J.R. Culham and M.M. Yovanovich
Microelectronics Heat Transfer Laboratory
Department of Mechanical Engineering
University of Waterloo
Waterloo, Ontario, Canada N2L 3G1

S. Lee
Aavid Engineering Ltd.
Laconia, NH

ABSTRACT

An analytically based model is presented for determining flow velocities and wall temperatures in system modules containing multiple printed circuit boards. The model provides a dynamic blending of two limiting solutions for two-dimensional, free convection channel flow, namely, a fully developed solution and an isolated plate solution. The effects of flow impediments, such as electro-magnetic containment screens, flow deflectors and baffles, on heat transfer within the module are incorporated to provide a better representation of practical applications. The solution procedure includes an implicit formulation for determining the heat transfer between channels based on local thermophysical characteristics, the contact resist ante between the heat sources and the printed circuit boards, and flow conditions. Results from the analytical models show good agreement with solutions and experimental data published in the open literature for a single channel with an uniform heat flux at each wall.

NOMENCLATURE

A	-	wall surface area, m^2
b	-	channel width, m
c_p		specific heat, J/kgK
9	-	gravitational acceleration, m/s^2
k	-	thermal conductivity, W/mK
ΣK_i	-	inlet, exit loss coefficients
L	-	channel length, m
Pr	-	Prandtl number
n		blending parameter
Nu_L	-	Nusselt number, $\equiv (qL)/(k(T_{max} - T_a))$
Nu_b	-	channel Nusselt number, $\equiv (qb)/(k(T_{max} - T_a))$
q	-	heat flux, W/m^2
Q		heat flow rate, W
r_1, r_2		heat flux ratio for left, right side
R		thermal resistance, $\equiv$ (AT/Q), K/W
$\mathrm{Ra}_L^\star$		modified Rayleigh number, $\equiv (g\beta q L^4 \mathrm{Pr})/(k\nu^2)$
$\mathrm{Ra}_b^\star$		channel Rayleigh number, $\equiv (g\beta q b^5 \mathrm{Pr})/(k\nu^2 L)$
Re_b		channel Reynolds number, $\equiv (\overline{u}b)/\nu$
T		temperature, K
AT		temperature difference, K
u		velocity in primary flow direction, m/s
W		channel depth, m
x		coordinate in primary flow direction, m
Y		coordinate normal to the channel wall, m

Greek Symbols

α	-	thermal diffusivity, m^2/s
β	-	volumetric expansion coefficient, K^{-1}
fs	-	hydraulic boundary layer thickness, m
δ_t	-	thermal boundary layer thickness, m
μ	-	dynamic viscosity, Ns/m^2
ν		kinematic viscosity, m^2/s
ρ	-	density, kg/m^3

Subscripts

a		ambient
c		contact
efj	-	effective
f	-	fluid
fd	-	fully developed
ap	-	isolated plate
j	-	junction
T	-	total
1)2	-	left and right surfaces

Superscripts

$-$		average
t		non-dimensional value

INTRODUCTION

Microelectronic systems can take several forms, ranging from the large cabinets found in mainframe computers or telecommunications equipment which contain several shelves of circuit boards, to small personal computers with a single board and optional plug-in expansion cards. Common to each of these systems is a need to know fluid temperatures and velocities as well as maximum board temperatures in order to accurately determine 'hot spots" on the circuit boards which could lead to reliability failures.

Modern telecommunications equipment is often designed using a modular approach, implementing natural convection cooling in place of its noisier and more costly forced convection counterpart. These system modules, as shown in Fig. 1, typically contain 2- 10 printed circuit cards suspended parallel to one another, thereby creating vertical channels cooled via buoyancy induced flow. In order to impede electro-magnetic interference between the module and other equipment, perforated metal screens are positioned at the fluid inlet and exit points.

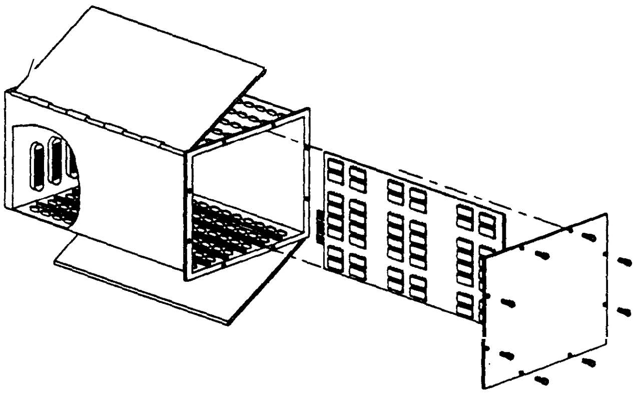

Fig. 1: Typical System Module With EMC Screens and Flow Diverters

These modules can be placed in a traditional tower arrangement, as shown in Fig. 2(a); however, as the fluid sink temperature increases from the lower to upper shelves within the system, the potential for heat dissipation is restricted and the overall thermal integrity of the system is jeopardized. Figure 2(b) illustrates one approach used to avoid this problem, where fresh, ambient air is introduced and heated air is directed out of each level by a system of baffles.

The addition of EMC screens and baffles to a flow-though module design introduces **a** restriction to the free flow of air and, in turn, has a detrimental effect on heat transfer. Even the presence of large objects on the circuit cards, such as packages or power supplies, may tend to restrict the free movement of the cooling &stream. Models are required that allow the designer to quickly and accurately determine the effects of these flow restrictions on the thermal performance of the system.

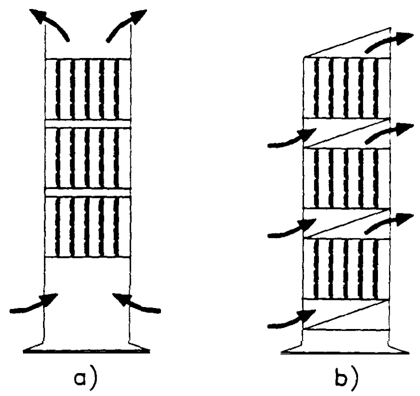

Fig. 2: System Flow Configurations: (a) Traditional Tower Arrangement, (b) Thermal Isolation Using Baffles

The problem involving laminar free convection in the region between vertically oriented, parallel plates has been examined by many researchers over the past fifty years. EIenbaas (1942) was the first to present an in-depth analysis of the channel problem for closely-spaced, isothermal plates, and his results are still considered a reference standard. Other researchers have since examined the isothermal problem, including Bodoia and Osterle (1962), Engel and Mueller (1967), Kettleborough (1971), and Quintiere and Mueller (1973).

Although the findings in these early works are significant, more appropriate models for determining the heat dissipation from printed circuit boards which use uniform heat flux boundary conditions have been suggested by other researchers.

Aung (1972) presented closed-form solutions for laminar free convection in vertical channels with unequal, uniform heat flux boundaries which experience fully-developed flow. Analytical expressions are developed for local fluid velocity and temperature distributions in terms of the relative magnitude of the heat flux between opposing channel walls. Aung, Fletcher, and Sernas (1972) performed numerical and experimental studies of developing laminar free convection in vertical, asymmetrically heated, parallel plate channels with uniform wall flux or uniform temperature boundary conditions. Although the many plots this work collectively provide a means of ascertaining the local wall temperature for many thermal and flow comp tions, this process would involve digitizing these plots and in general, it is not possible to obtain local values from ' numerical solutions for arbitrary thermal conditions.

Miyatake and Fujii (1974) developed an analytical model for laminar free convection between two plates with unequal, uniform heat fluxes. Their based on a combination of a fully-developed flow tote and natural convection from a single, vertical was compared with numerical values for a wid Prandtl numbers and with experimental data The resulting~ expressions for local Nusselt numbe to predict local plate temperatures for a wide range of channel configurations.

Experimental results for free convection between vertical plates with symmetric, uniform flux heating are presented by Wirtz and Stutzman (1982). The authors developed an expression for the maximum wall temperature based on the blending of fully-developed channel flow and isolated plate, natural convection asymptotes. This blended solution is validated using measured values of local temperature.

Bin-Cohen and Rohsenow (1984) developed analytical expressions for the Nusselt number for symmetrically and asymmetrically heated isothermal and isoflux channels, as well as a set of equations designed to optimize the spacing between adjacent circuit boards.

Although each of these references present valuable insight into the channel flow problem, none of the resulting expressions for wall temperature can be easily modified to include the effects of flow-restricting devices, such as electro-magnetic containment (EMC) screens, flow deflectors or baffles. As well, none of the previous works have addressed the issue of heat transfer between adjacent channels.

The following work presents a model for predicting local wall temperatures and average fluid exit velocities for systems of arbitrarily arranged and asymmetrically heated parallel plates. The solution procedure is based on a blending of the asymptotic solutions for fully-developed, two-dimensional channel flow and natural convection from an isolated flat plate. The model includes algorithms for calculating the distribution of heat between the channels as a function of the case/board thermal resistances. Validation of the model will be presented using previously published results and numerical simulations from a commercial, finite volume based CFD code.

MODEL DESCRIPTION

Blended Solution Method. In designing a system module which depends on free convection cooling, the thermal analyst requires both surface temperatures (to predict component and board temperatures) and average fluid velocity and temperature (to determine the cooling capacity of the natural convection flow). The behavior of these quantities has been well documented for both of the limiting cases, fully-developed channel flow between parallel plates and natural convection from a single, vertical plate.

In the case of long, narrow channels with small values of heat flux, the flow in the channel quickly becomes fully-developed. Within a fully-developed, forced convection flow, the velocity profile assumes a parabolic shape, the average fluid velocity is constant, and the fluid temperature at the wall increases linearly along the length of the channel.

The other limiting case involves short, wide channels with large heat fluxes at the wall, where the flow continues to develop from the entrance to the exit. If the thermal and hydrodynamic boundary layers associated with each side of the channel do not interact before the channel exit, then the heat transfer at each wall begins to resemble that of an isolated flat plate in a quiescent fluid.

In the intermediate region between these two asymptotes, the flow entering the channel develops until the boundary layers interact. As the flow fields on each side of the channel continue to develop, the core velocity increases until the fully-developed profile is reached. It is apparent that the behavior of the channel in this intermediate region can be described by some combination of the limiting cases.

The proposed model uses a blending technique presented by Churchill and Usagi (1972) to combine the information from each asymptote into an explicit expression that predicts the behavior of the solution in the intermediate region. This blending technique has been successfully used by a number of researchers for a variety of solutions, including mixed convection (Lee, Culham, and Yovanovich, 1991) and transient heat conduction (Yovanovich, Teertstra, and Culham, 1994), as well as Wirtz and Stutzman (1982), Bar-Cohen and Rohsenow (1984) and Churchill (1977) for their analysis of this channel flow problem. The present work will demonstrate the development of blended solutions for both the Nusselt number and the non-dimensionalized average exit velocity.

Average Exit Velocity. In order to effectively model the average fluid velocity across the exit of the channel using a blended solution, it is necessary to define the following dimensionless quantity:

$$\overline{u}' = \frac{\overline{u} \cdot \delta_{eff}}{\nu} \tag{1}$$

This non-dimensional exit velocity $\overline{u}'$ is determined using the average exit velocity and an effective boundary layer thickness, δ_{eff}, defined as the thickness of the fluid layer at the exit that contributes to the buoyant flow. For the case of a long, narrow channel with small heat fluxes, the average velocity $\overline{u}$ is analogous to the forced convection bulk velocity and δ_{eff} is reduced to half of the channel width, $b/2$. At the other limit, where the channel is wide and short with large values of heat flux, $\overline{u}$ is defined as the average velocity across the hydrodynamic boundary layer and δ_{eff} is the thermal boundary layer thickness (it is assumed for this analysis that $Pr \approx 1$, such that $\delta = \delta_t$). For this isolated plate, natural convection case, multiplying the average velocity in the boundary layer by $\delta_{eff}/(b/2)$ assumes that fluid movement occurs only within the boundary layer and the velocity in the core region between the boundary layers is zero.

The general form of the blended solution for the average

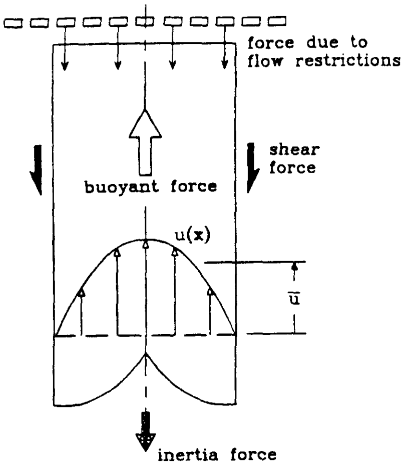

Fig. 3: Schematic of Force Balance in Fully Developed Channel Flow

exit velocity is as follows:

$$\overline{u}' = \frac{1}{\left[\left(\frac{1}{\overline{u}'_{fd}}\right)^n + \left(\frac{1}{\overline{u}'_{ip}}\right)^n\right]^{1/n}} \qquad (2)$$

where $\overline{u}'_{fd}$ is the dimensionless average exit velocity asymptote for fully-developed flow and $\overline{u}'_{ip}$ is the asymptote for natural convection from an isolated plate. These asymptotes are determined in the following sections.

Fully-Developed Flow. The fluid velocity within a fully-developed channel is a constant value, easily determined by simple force and energy balances on the control volume shown in Fig. 3:

Buoyant Force = Shear Force + Flow Restrictions

Power Dissipated = Net Enthalpy Transport

The force balance for the channel formed between two vertical, uniformly heated parallel plates can be stated in terms of the channel width, b, length, L, and depth, W:

$$\rho g\beta(bW)\int_0^L \Delta\overline{T}(x)\; dx = \mu(2LW)\left.\frac{\partial u}{\partial y}\right|_{y=wall} + (\Sigma K_i + 1)\rho(bW)\frac{\overline{u}^2}{2} \qquad (3)$$

where the overall loss coefficient ΣK_i is a summation of the K factors that describe pressure losses induced by flow restrictions due to EMC screens, blockage effects, and large-scale surface roughness. The change of the average temperature of the fluid, $\Delta\overline{T}(x)$, is determined using the enthalpy balance:

$$q_1(1+r_1)(xW) = \rho c_p(bW)\Delta\overline{T}(x)\overline{u}$$

$$\Delta\overline{T}(x) = \frac{q_1(1+r_1)\,x}{\rho c_p b\overline{u}} \qquad (4)$$

where the heat flux ratio r_1 is introduced for cases where the heat flux at the left and right sides of the channel, q_1 and q_2, are different:

$$r_1 = \frac{q_2}{q_1} \qquad (5)$$

Using a parabolic velocity profile for fully developed flow the wall shear can be easily determined:

$$\left.\frac{\partial u}{\partial y}\right|_{y=0} = \left.\frac{\partial}{\partial y}\left(6\overline{u}\,\frac{y}{b}\left(1-\frac{y}{b}\right)\right)\right|_{y=0} = \frac{6\overline{u}}{b} \qquad (6)$$

By substituting the wall shear and average temperature rise into Eq. (3) and simplifying, the following polynomial expression is formed:

$$\left[(\Sigma K_i + 1)\frac{\rho b}{2}\right]\overline{u}^3 + \left[\frac{12\mu L}{b}\right]\overline{u}^2 - \left[\frac{2g\beta q_1(1+r_1)L^2}{c_p}\right] = 0 \qquad (7)$$

This polynomial expression can be solved using an iterative root-finding technique, such as the Newton-Raphson method. Because the value corresponding to the average channel velocity will always be the largest positive root of Eq. (7), the initial "guess" for the Newton-Raphson iteration should be a velocity that is much larger than any possible solution, i.e. $u = 10\ m/s$.

At the fully-developed flow limit, the effective boundary layer thickness is reduced to half the channel width:

$$\delta_{eff} = b/2$$

and the non-dimensions.lized exit velocity can be determined by:

$$\overline{u}' = \frac{\overline{u}b}{2\nu} \qquad (8)$$

where $\overline{u}$ is determined by Eq. (7).

Isolated Plate, Natural Convection. The average fluid velocity within the hydrodynamic boundary layer at the end of an isolated, uniformly heated, vertical plate is available through a solution of the integral formulations of the momentum and energy equations:

$$\frac{d}{dx}\int_0^\delta u^2\,dy = g\beta\int_0^\delta (T - T_a)\,dy - \nu\left.\frac{\partial u}{\partial y}\right|_{y=0} \qquad (9)$$

$$\frac{d}{dx}\int_0^{\delta_t} u\,(T - T_a)\,dy = -\alpha\left.\frac{\partial T}{\partial y}\right|_{y=0} \qquad (10)$$

where an isoflux boundary condition is imposed at $y = 0$. Assuming Pr ≈ 1, such that $\delta_t = \delta$, and neglecting the effects of flow restrictions results in the following expressions for the velocity and boundary layer thickness at the channel exit:

$$u(L,\delta) = 75\alpha\left(\frac{1}{450(1+\Pr)}\frac{g\beta q_1 L^{3/2}}{k\alpha^2}\right)^{2/5}\frac{y}{\delta}\left(1-\frac{y}{\delta}\right)^2$$

$$\delta(L) = \left(450(1+\Pr)\frac{k\alpha^2}{g\beta q_1 L}\right)^{1/5}$$

The average velocity within the boundary layer is available through an integration of the velocity profile over the boundary layer thickness:

$$\bar{u} = \frac{1}{\delta}\int_0^{\delta} u(\delta)\,dy = \frac{75\alpha}{12}\left(\frac{1}{450(1+\mathrm{Pr})}\frac{g\beta q_1 L^{3/2}}{k\alpha^2}\right)^{2/5} \tag{13}$$

At the isolated plate limit, the effective boundary layer thickness approaches the thermal boundary layer thickness predicted by the integral solution, and the nondimensionalized velocity across the left side of the channel exit becomes:

$$\bar{u}' = \frac{\bar{u}\delta}{\nu} = \frac{25}{4\mathrm{Pr}}\left[\frac{\mathrm{Pr}}{450(1+\mathrm{Pr})}\mathrm{Ra}_L^*\right]^{1/5} \tag{14}$$

where:

$$\mathrm{Ra}_L^* = \frac{g\beta q_1 L^4}{k\nu^2}\,\mathrm{Pr} \tag{15}$$

In a similar fashion, the average exit velocity over the right side of the channel can be determined by Eq. (14) using:

$$\mathrm{Ra}_L^* = \frac{g\beta q_2 L^4}{k\nu^2}\,\mathrm{Pr} \tag{16}$$

Average Exit Velocity Model Summary. Combining the formulations for the asymptotes at each side of the channel, Eqs. (8) and (14), into the general expression, Eq. (2), yields blended solutions for the average exit velocity: for the left side of the channel:

$$\bar{u}' = \frac{1}{\left[\left(\frac{2\nu}{b\bar{u}_{fd}}\right)^n + \left(\frac{\mathrm{Pr}^4(1+\mathrm{Pr})}{21.193}\frac{1}{Ra_L^*}\right)^{n/5}\right]^{1/n}} \tag{17}$$

where $\bar{u}_{fd}$ is the largest positive root of the polynomial expression resulting from the force balance, Eq. (7), and Ra_L^* is calculated using q_1 and q_2 for the left and right sides of the channel, respectively. By assuming that the velocity in the core region between the effective boundary layers is zero, the average velocity across each side of the channel can be calculated by:

$$\bar{u} = \frac{1}{b/2}\left(\frac{\bar{u}'\nu}{\delta_{eff}}\delta_{eff}\right) \tag{18}$$

The resulting expression for the average exit velocity for left and right sides of the channel is:

$$\bar{u} = \frac{2\nu}{b}\cdot\left[\left(\frac{2\nu}{b\bar{u}_{fd}}\right)^3 + \left(\frac{\mathrm{Pr}^4(1+\mathrm{Pr})}{21.193}\frac{1}{Ra_L^*}\right)^{3/5}\right]^{-1/3} \tag{19}$$

where the blending parameter $n = 3$ is chosen based on the direct relationship between Nu and $\bar{u}$ at the fully developed limit, as described in the following section.

Maximum Board Temperature. The maximum temperature difference between the fluid adjacent to the channel wall and the ambient "is available through the Nusselt number, defined for this problem as:

$$\mathrm{Nu}_L = \frac{qL}{k(T_{max} - T_a)} \tag{20}$$

where q *is* the heat flux at the wall and T_{max} and T_a *are* maximum wall and ambient temperatures, respectively. The blended solution for local Nusselt is:

$$\mathrm{Nu}_L = \frac{1}{\left[\left(\frac{1}{\mathrm{Nu}_{fd}}\right)^n + \left(\frac{1}{\mathrm{Nu}_{ip}}\right)^n\right]^{1/n}} \tag{21}$$

where Nu_{fd} is the Nusselt number asymptote for fully developed flow and Nu_{ip} is the asymptote for natural convection from an isolated plate. Each of these asymptotes is developed in the following sections.

Fully-Developed Flow. If the Nusselt number is defined using the local average temperature, 7(z), rather than the ambient temperature, *T.*, it becomes a constant for fully-developed channel flow (Arpaci and Larsen, 1984):

$$\mathrm{Nu}_b = \frac{qb}{2k(T_w(x) - \overline{T}(x))} = \frac{35}{17} \tag{22}$$

In order to convert this result in terms of the ambient temperature, an enthalpy balance is performed over the length L of the channel:,

$$\begin{aligned}(Q_1 + Q_2) &= \dot{m}c_p\left(\overline{T}(x = L) - T_a\right)\\ &= \rho c_p(bW)\left(\overline{T}(x = L) - T_a\right)\bar{u}_{fd}\end{aligned} \tag{23}$$

where $\bar{u}_{fd}$ is the average velocity across the channel and Q_1 and Q_2 are the total heat applied to the left and right sides of the channel, respectively. By introducing the heat flux ratios r_1 and r_2, the total heat dissipated in the channel can be expressed as:

$$(Q_1 + Q_2) = q_1(1 + r_1)(LW) \tag{24}$$

$$= q_2(1 + r_2)(LW) \tag{25}$$

where:

$$r_1 = \frac{q_2}{q_1} \qquad r_2 = \frac{q_1}{q_2}$$

Substituting the energy balance stated in terms of q_1 into Eq. (22) for the channel exit, $x = L$, *gives:*

$$\frac{q_1 b}{2k\left(T_{max} - \frac{q_1(1+r_1)\alpha L}{bk\bar{u}_{fd}} - T_a\right)} = \frac{35}{17} \tag{26}$$

Rearranging this equation in terms of the Nusselt number formulation in Eq. (20) yields the following:

$$\mathrm{Nu}_L = \frac{\frac{70}{17}}{\left(\frac{b}{L} + \frac{70}{17}\cdot\frac{(1+r_1)\alpha}{b\bar{u}_{fd}}\right)} \tag{27}$$

In order to forma proper blended solution, each portion of the solution must be an asymptote. This requires that the behavior of Eq. (27) be examined at the limits:

$$L \rightarrow \infty$$

At the fully-developed limit, the first term in the denominator of Eq. (27) is negligible in comparison to the second term. Therefore, the fully developed asymptote for the local Nusselt number becomes:

$$\mathrm{Nu}_{fd} = \frac{b\,\overline{u}}{(1+r_1)\alpha} \tag{28}$$

for the left side of the channel and:

$$\mathrm{Nu}_{fd} = \frac{b\,\overline{u}}{(1+r_2)\alpha} \tag{29}$$

for the right side. The fully developed average velocity $\overline{u}$ is determined using Eq. (7), as described in the previous section.

Isolated Plate, Natural Convection. At this limit it is assumed that the average fluid velocity within a wide channel is small enough that the flow restrictions caused by various components in the system module are negligible. This approximation would allow the use of a standard solution for the local Nusselt number for the isoflux flat plate, such as the sirnilarity solution of Sparrow and Gregg (1956). However, as noted by a number of researchers including Bar-Cohen and Rohsenow (1984), Aung et al. (1972), Wirtz and Stutzman (1982), and Sobel et al. (1966),- measured data seems to suggest that the use of& isolated plate solution will underpredict the Nusselt number by as much as 15% for large Rayleigh numbers. Each of these authors have recommended that the coefficient C in the asymptote:

$$\mathrm{Nu}_{ip} = C\,\mathrm{Ra}_L^{\star\,1/5} \tag{30}$$

be larger than the value C = 0.529 predicted by the Sparrow and Gregg (1956) solution for Pr = 0.7. Aung et al. (1972) and Wirtz and Stutzman (1982) use the same value, C = 0.577, while Sobel et al. (1966) recommends C = 0.583. The largest value is that used by Bar-Cohen and Rohsenow (1984), C = 0.6355. Because of the significant discrepancies between these values and the wide range of experimental results, **a** combination of these limits is chosen, such that:

$$\mathrm{Nu}_{ip} = 0.6\,\mathrm{Ra}_L^{\star\,1/5} \tag{31}$$

where:

$$\mathrm{Ra}_L^\star = \frac{g\beta q_1 L^4}{k\nu^2}\cdot \mathrm{Pr} \tag{32}$$

$$\mathrm{Ra}_L^\star = \frac{g\beta q_2 L^4}{k\nu^2}\cdot \mathrm{Pr} \tag{33}$$

for the left and right sides of the channel, respectively.

Because these expressions are not dependent on the channel spacing, it is already an asymptote for the blended solution and it requires no modification.

Maximum Board Temperature Model Summary. By combining the formulations for the asymptotes, Eqs. (28) and (31), into the general expression, Eq. (21), the blended solution for the local Nusselt number becomes:

$$\mathrm{Nu}_L = \frac{1}{\left[\left(\frac{(1+r_1)\alpha}{b\,\overline{u}_{fd}}\right)^n + \left(\frac{1}{0.6\,Ra_L^\star}\right)^{n/5}\right]^{1/n}} \tag{34}$$

where $\overline{u}_{fd}$ is the fully-developed velocity asymptote, calculated using Eq. (7) from the previous section.

A blending parameter of n = 3 for Eq. (21) has been recommended both by Lee, Culham and Yovanovich (1991) based on their **work** involving a blended solution for mixed convection, and by Wirtz and Stutzman (1982). Therefore, the maximum fluid temperature along surface 1 at the channel exit is determined by:

$$T_{max} = \frac{q_1 L}{k}\left[\left(\frac{(1+r_1)\alpha}{b\,\overline{u}_{fd}}\right)^3 + \left(\frac{1}{0.6\,\mathrm{Ra}_L^\star}\right)^{3/5}\right]^{1/3} + T_a \tag{35}$$

and along surface 2 using:

$$T_{max} = \frac{q_2 L}{k}\left[\left(\frac{(1+r_2)\alpha}{b\,\overline{u}_{fd}}\right)^3 + \left(\frac{1}{0.6\,\mathrm{Ra}_L^\star}\right)^{3/5}\right]^{1/3} + T_a \tag{36}$$

where Ra* is calculated using **Eqs. (32) and (33).**

Heat Transfer Between Channels. The heat tranafer analysis presented in the previous section was based on an isolated channel where all heat flows are into the control volume formed between opposing channel walls. The **back** side of each wall is assumed to be adiabatic. However, **the** printed circuit boards forming the walls in most **micro**-electronics systems are conductive and heat is **transferred** between adjacent channels which, in turn, influences **the** buoyancy driven fluid flows.

Figure 4 shows the schematic representation of the **heat** flow paths in the cross section of a typical printed **cir**-cuit board. When the board is fully populated with heat sources, the predominant direction for heat flow is directly from the sources to the surrounding fluid sink, denoted as T_{a_1} and T_{a_2}, or along a normal path through the board to the fluid sink on its back-side. By assuming that heat flow in the plane of the circuit board is minimal in relation to the heat flow across the thickness of the board, a simple thermal network can be established based on a series path through the cross section of the board, as shown in Fig. Two thermal resistances must be considered at each heat source; first, the fluid resistance between the heat source and the surrounding fluid sink, denoted as R_f, and end, the contact resistance between the heat source the printed circuit board, denoted as R_c.

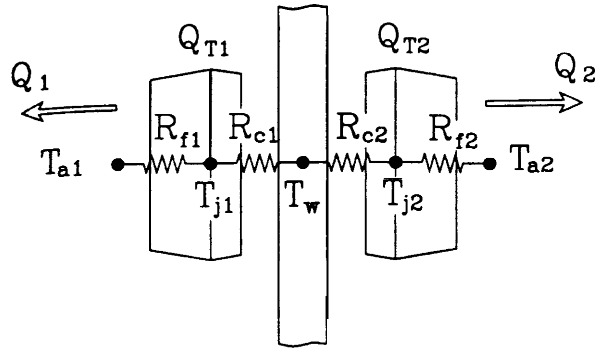

Fig. 4: Thermal Resistance Network at Channel Walls

Applying the blended solution for the Nusselt number developed in the previous section, Eq. (34), the thermal resistance between the heat source junction and the ambient can be determined using:

$$
\begin{aligned}
R_{f1} &= \frac{T_{j1} - T_{a1}}{Q_1} \\
&= \frac{1}{kW}\left[\left(\frac{(1+r_1)\alpha}{b\,\overline{u}_{fd}}\right)^3 + \left(\frac{1}{0.6\,Ra_L^\star}\right)^{3/5}\right]^{1/3} \qquad (37)\\
R_{f2} &= \frac{T_{j2} - T_{a2}}{Q_2} \\
&= \frac{1}{kW}\left[\left(\frac{(1+r_2)\alpha}{b\,\overline{u}_{fd}}\right)^3 + \left(\frac{1}{0.6\,Ra_L^\star}\right)^{3/5}\right]^{1/3} \qquad (38)
\end{aligned}
$$

where $Ra_L^\star$ is calculated using q_1 and q_2 for surfaces 1 and 2, respectively.

The introduction of a contact resistance at the interface between the heat source junction and the printed circuit board poses a problem in which three nodal temperatures, T_w, T_{j1} and T_{j2}, must be known in order to ascertain the heat flow rate from each side of the wall. Because the problem is indeterminate and cannot be solved directly, it will be recast in the form of two specific cases where, because of the linearity of the energy equation, the sum of the solutions to the two cases is the solution to the original problem. These cases are presented in the following sections.

Case 1: $Q_{T1} = 0$. In this first case, the heat distribution is determined based on Q_{T2} being the active heat source. An expression for the total heat flow rate, Q_{T2}, can be written based on the resistance network shown in Fig. 4:

$$Q_{T2} = Q_1 + Q_2 = \frac{T_{j2} - T_{a1}}{R_{f1} + R_{c1} + R_{c2}} + \frac{T_{j2} - T_{a2}}{R_{f2}} \qquad (39)$$

By assuming a parabolic temperature distribution in the channels, the mean ambient temperature can be written as a function of a mixed channel bulk temperature and the junction temperature, as:

$$
\begin{aligned}
T_{a1} &= \frac{3}{2}\overline{T}_1 - \frac{1}{2}T_{j1} \qquad (40)\\
T_{a2} &= \frac{3}{2}\overline{T}_2 - \frac{1}{2}T_{j2} \qquad (41)
\end{aligned}
$$

If *we* note that:

$$T_{j1} = T_{j2} - Q_1(R_{c_1} + R_{c_2}) \qquad (42)$$

then combining Eq. (39) with Eqs. (40) - (42) gives the heat flow rate from surface 1, Q_1, as a fraction of the total heat dissipation:

$$\frac{Q_1}{Q_{T2}} = \frac{(2/3)R_{f2} + (\overline{T}_2 - \overline{T}_1)/Q_{T2}}{(2/3)(R_{f1} + R_{f2}) + (R_{c_1} + R_{c_2})} \qquad (43)$$

The heat flow from surface 2 for case 1 *can* be easily determined using an energy balance:

$$\frac{Q_2}{Q_{T2}} = 1 - \frac{Q_1}{Q_{T2}} \qquad (44)$$

Case 2: $Q_{T2} = 0$. In this second case, the heat distribution among the neighboring channels is determined using Q_{T1} as the active heat source. The analysis in Case 1 can be repeated with subscripts 1 and 2 interchanged to obtain an expression for the heat flow rate fraction as a function of Q_{T1}.

$$Q_1\left((2/3)R_{f1}\right) + T_1 = Q_2\left((2/3)R_{f2} + (R_{c_1} + R_{c_2})\right) + \overline{T}_2 \qquad (45)$$

With $Q_{T1} = Q_1 + Q_2$, Eq. (45) can be rearranged to yield:

$$\frac{Q_1}{Q_{T1}} = \frac{(2/3)R_{f2} + (R_{c_1} + R_{c_2}) + (\overline{T}_2 - \overline{T}_1)/Q_{T1}}{(2/3)(R_{f1} + R_{f2}) + (R_{c_1} + R_{c_2})} \qquad (46)$$

which represents the relative portion of Q_{T1} that is dissipated into channel side 1.

Superposition of Case 1 and Case 2. The general case of a channel wall with heat sources on each side can be solved by superimposing the solutions presented in Case 1 and Case 2. The overall heat flow rate from side 1 is the sum of Q_1 from Eq. (43) and Q_1 from Eq. (46). Q_2 is then the difference between the total Q_1 and the total heat dissipation $Q_{T1} + Q_{T2}$.

MODEL VALIDATION

Validation of the various portions of the model developed in the preceding section are performed using solutions and measured data from the literature as well as results generated by FLOTHERM (1994), a finite volume based CFD code.

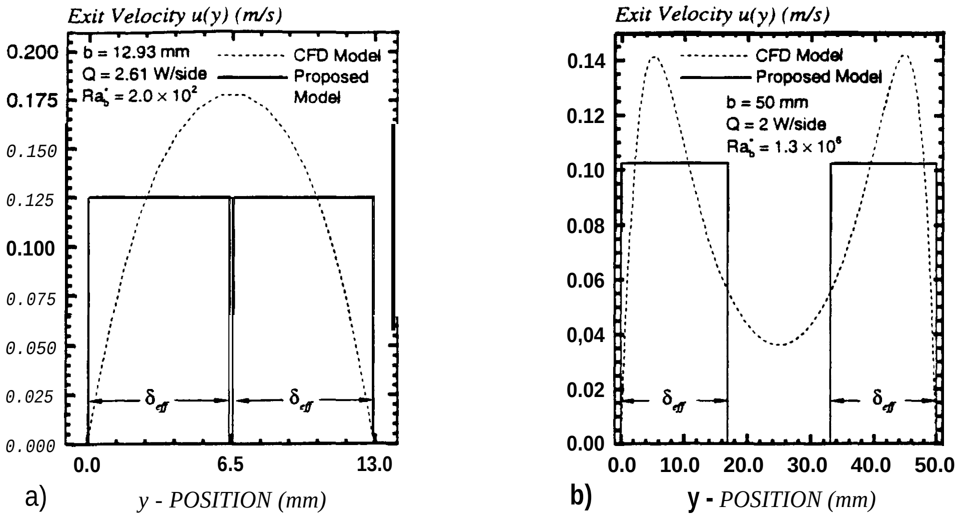

Fig. 5: Comparison of Exit Velocity Profiles: (a) Fully Developed Flow, (b) Wide Channel Spacing

Average Exit Velocity. In order to better illustrate the concept of the effective boundary layer thickness as it is applied in the proposed model for the average exit velocity, outlet velocity profiles for two limiting cases are examined in detail. Velocity profiles are generated using FLOTHERM for a fully developed case, with $b = 12.93mm$ and Q = 2.61 W/side, such that the channel Rayleigh number is near its *lower limit*, $Ra_b^* = 200$, *and* for a case approaching isolated plate behavior, $b = 50mm$, Q = 2W/side, such that Ra_b^* = 1.3 x 10^6. These velocity profiles are compared to the model in Fig. 5, where the transition of the effective boundary layer thickness δ_{eff} between its limits of $b/2$ and δ_t is clearly demonstrated.

The average exit velocity calculation is validated for a wide range of Rayleigh numbers using FLOTHERM results and measured values from Fujii et al. (1994), as shown in Fig. 6. In order to compare these results, it is convenient to non-dimensionalize the average exit velocity using the channel Reynolds number:

$$Re_b = \frac{\overline{u}b}{\nu} \qquad (47)$$

and the aspect ratio b/L.

As can be seen from Fig. 6, the model has excellent agreement with both the CFD results and the measured values for the cases Ra < 10^4. However, at the higher Rayleigh numbers, the model begins to underpredict the numerical values. This can be explained by examining the assumption that the fluid outside the boundary layers has a velocity of u = *Ore/s, as* described by Eq. (18) and demonstrated by Fig. 5 (b). This simplification introduces inaccuracy into the model for channels in the intermediate region, $Ra_b^* \approx 10^5 - 10^6$, leading to an underprediction of the average exit velocity by 10-15 % for these cases. However, through the enthalpy balance this lower velocity leads to an over-prediction of the average fluid temperature, a consistent conservative estimate useful for most thermal analyses.

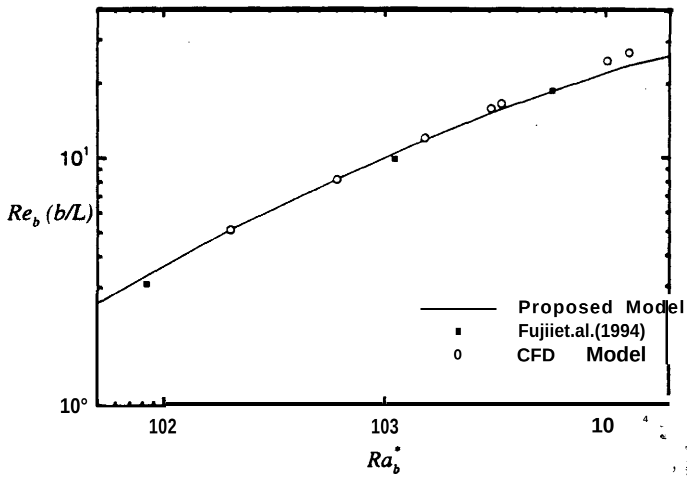

Fig. 6: Average Exit Velocity Model Validation

Maximum Board Temperature. In Fig. ? the blended solution for the Nusselt number is compared both to the models of Wirtz and Stutzman (1982), Miyatake and Fujii (1974) and Bar-Cohen and Rohsenow (1984), and to the measured values presented by Johnson (1986) for a single, symmetrically heated channel with Rayleigh number in the range 1 < Ra_b^* < 10^5. As can be seen from this figure, the blended solution has excellent agreement with the existing models for the symmetrically heated isoflux channel over the fidl range of channel spacings and heat flux values. The proposed model also accurately predicts the majority of the measured data reported by Johnson (1986), where the scatter of the data in the 10 < Ra_b^* < 100 can be attributed to variations in experimental apparatus from smooth boards to actual circuit cards with packages.

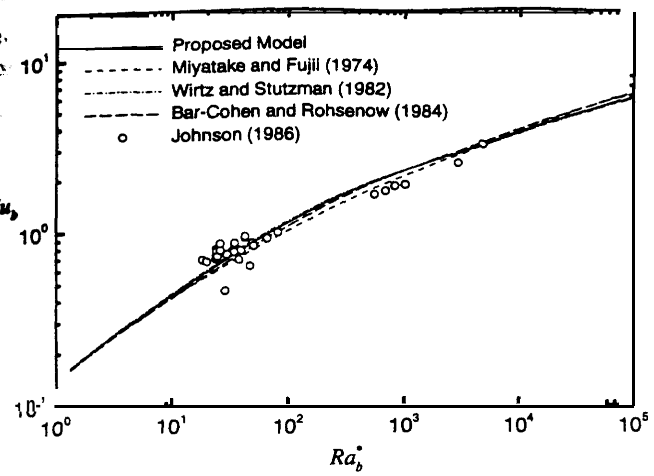

Fig. 7: **Nu_b Model** Validation for Symmetric Channel

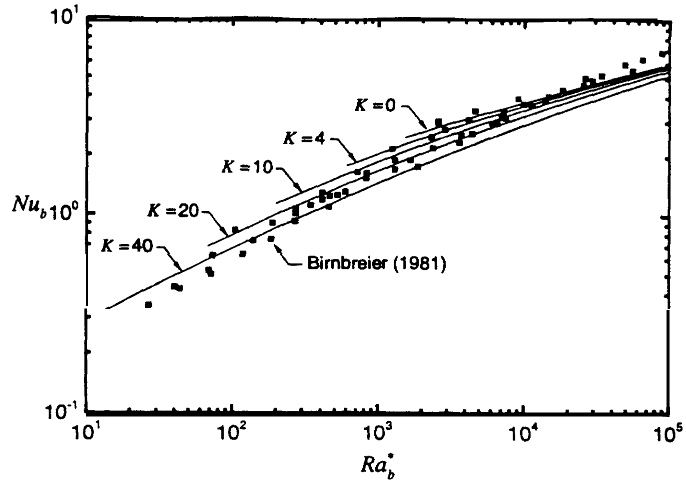

Fig. 8: Effects of Flow Restrictions on $\mathbf{Nu_b}$ vs. $\mathbf{Ra_b^*}$

The effects of flow restrictions on the solution for the Nusselt number are examined more closely using the experimental results presented by Birnbreier (1981). Figure 8 presents these measured values and several solutions using flow restriction values between $K = O$ and $K = 40$ *in* terms of the channel Rayleigh number for the range $10 < \mathbf{Ra_b^*} < 10^5$. The apparatus used by Birnbreier (1981) was constructed to represent an actual thermal module, with blockages at the inlet and outlet that reduced the air flow cross section to about 65 %. Using a simple model for the flow restriction caused by a narrowed section in a uniform channel (Idelchik, 1994), this 6570 open area can be shown to correspond to $K \approx 4$. In addition to these entrance and exit flow restrictions, ***8mm*** thick teflon blocks were attached to the boards at various locations in order to simulate the blockage effects of large packages or connectors. The effects of adding these packages varies as a function of the channel spacing, with little effect for $Ra > 10^4$ and larger effects for smaller values. At the lower limit, where channel spacing is reduced to ***13.6mm,*** these ***8mm*** blocks have a substantial impact on the solution, as reflected by the flow restriction parameter $K = 40$ shown in Fig. 8.

CONCLUSIONS

An analytically based model for determining fluid velocities and wall temperatures in system modules containing multiple printed circuit cards has been developed. The circuit boards are modeled as uniformly heated, vertically-oriented parallel plates and the solutions are blended combinations of fully-developed channel flow and isolated plate, natural convection asymptotes. This proposed solution includes flow restriction factors which can be used to model the effects of EMC screens, flow diverters and baffles, and flow blockages. The multi-channel model also includes an algorithm for determining the heat distribution between adjacent channels for cases involving asymmetric heating.

Good agreement has been demonstrated between the blended solution for the Nusselt number and existing models and experimental values from the open literature for a wide range. of channel spacings and heat flux values. The blended solution for the average exit velocity, when compared numerical results and the available measured values, also showed good agreement. Finally, the effects of the *K* factor have been examined using measured data for variety of simulated flow restrictions.

ACKNOWLEDGMENTS

The authors gratefully acknowledge support of both the Natural Sciences and Engineering Research Council of Canada under Operating Grant No. 661-069/91 and Bell Northern Research, Kanata, Ontario, Canada. The financial support of the Manufacturing Research Corporation of Ontario is also greatly appreciated.

REFERENCES

Arpaci, V.S. and Larsen, P. S., 1984, Convection Heat *Transfer,* Prentice-Hall, Inc., Englewood Clifs, NJ.

Aung, W., 1972, "Fully Developed Larninar Free Convection Between Vertical Plates Heated Asymmetrically," *Int. J. Heat Mass Transfer,* Vol. 15, pp. 1577-1580.

Aung, W., Fletcher, L. S., and Sernas, V., 1972, "Developing Larninar Free Convection Between Vertical Flat Plates With Asymmetric Heating," *Int. J. Heat Mass Transfer,* Vol. **15,** pp. 2293-2308.

Bar-Cohen, A. and Rohsenow, W. M., 1984, "Thermally Optimum Spacing of Vertical, Natural Convection Cooled, Parallel Plates," *ASME Journal of Heat Transfer,* Vol. 106, pp. 116-123.

Birnbreier, H., 1981, "Experimental Investigations on the Temperature Rise of Printed Circuit Boards in Open Cabinets with Natural Ventilation," *ASME Heat Transfer in Electronic Equipment,* M.D. Kelleher and M.M.

Yovanovich, eds., HTD Vol. 20, pp. 19-23.

Bodia, J.R. and Osterle, J. F., 1962, 'The Development of Free Convection Between Heated Vertical Plates," *ASME Journal of Heat Transfer,* Vol. 84C, pp. 40-44.

Churchill, S. W., 1977, 'A Comprehensive Correlating Equation for Buoyancy-Induced Flow in Channels," *Letters in Heat and Mass Transfer,* Vol. 4, pp. 193-199.

Churchill, S.W. and Usagi, R., 1972, 'A General Expression for the Correlation of Rates of Transfer and Other Phenomena," *AIChE Journal,* Vol. 18, No. 6, pp. 1121-1128.

Elenbaas, W., 1942, 'Heat Dissipation of Parallel Plates by Free Convection," *Physics,* Vol. 9, pp. 1-28.

Engel,R.K. and Muelller, W. K., 1967, 'An Analytical Investigation of Natural Convection in Vertical Channels," *ASME* Paper 67-HT- 16.

FLOTHERM, 1994, FLOMERICS Inc., 57 East Main St., Westborough, MA, 01581.

Fujji, M., Tornimura, T., Zhang, X., and Gima, S., 1994, "Natural Convection From an Array of Vertical Parallel Plates," Proc. 1994 International Heat Transfer Conference, Vol. 7, pp. 49-54.

Idelchik, I. E., 1994, *Handbook of Hydraulic Resistance,* CRC Press, Boca Raton, FL.

Johnson, C. E., 1986, "Evaluation of Correlations for Natural Convection Cooling of Electronic Equipment," *ASME Heat Transfer in Electtonic Equipment,* A. Bar-Cohen, cd., HTD Vol. 57, pp. 103-111.

Kettleborough, C. F., 1971, 'Transient Larninar Free Convection Between Heated Vertical Plates Including Entrance Effects," *Int. J. Heat Mass Transfer,* VOL 15, pp. 883-896.

Lee, S., Culham, J. R., and Yovanovich, M. M., 1991, "Parametric Investigation of Conjugate Heat Transfer From Microelectronic Circuit Boards Under Mixed Convection Cooling," 1991 International Electronic Packaging Conference, San Diego, California, September 15-19.

Miyatake, O. and Fujii, T., 1974, 'Natural Convective Heat Transfer Between Vertical Parallel Plates With Unequal Heat Fluxes,* *Heat Transfer - Japanese Research 3-3, pp. 29-33.*

Quintiere, J. and Mueller, W.K., 1973, "An Analysis of Laminar Free and Forced Convection Between Parallel Plates," *ASME Journal of Heat Transfer,* Vol. 95, pp. 53-59.

Sobel, N., Landis, R., and Mueller, J. R., 1966, 'Natural Convection Heat Transfer in Short Vertical Channels Including the Effects of Stagger," ***Proc. International Heat*** *Transfer Conference,* pp. 121-125.

Sparrow, E.M. and Gregg, J. L., 1956, "Laminar free Convection From a Vertical Plate With Uniform Surface Heat Flux," Trans. *ASME,* Vol. 78, pp. 435-440.

Wirtz, R.A. and Stutzman, R. J., 1982, 'Experiments on Free Convection Between Vertical Plates With Symmetric Heating," *J. Heat 7ransfer,* Vol. 104, pp. 501-507.

Yovanovich, M. M., Teertstra, P. and Culham, J. R., 1994, 'Modeling Transient Conduction From Isothermal Convex Bodies of Arbitrary Shape," AIAA/ASME 6th Thermophysics and Heat Transfer Conference, Colorado Springs, CO, June 20-23.